GEOPHYSICAL RESEARCH LETTERS, VOL. 27, NO. 19, PAGES 3153-3156, OCTOBER 1, 2000

A Gyrophase-Bunched Electron Signature Upstream of the Earth's Bow Shock

C. Gurgiolo

Bitterroot Basic Research Inc., Hamilton, MT

D. Larson, and R. P. Lin

University of California at Berkeley, Berkeley, CA

H. K. Wong

Aurora Sciences, San Antonio, TX

Abstract. A possible sustained signature of a gyrophase-bunched electron distribution just upstream of the Earth's bow shock is presented. The data, obtained by the ISTP WIND 3-D Plasma and Energetic Particle Experiment, show several clear examples of a non-gyrotropic, energetic electron distribution moving into the upstream. The signature is probably that of a locally phase-trapped electron distribution.

Introduction

To date only one observational paper exists in the literature on non-gyrotropic electron distributions upstream of the Earth's bow shock [*Anderson et al.*, 1985]. Contrast this to the large number of similar papers on gyrophase bunched ions in the upstream region (*Thomsen*, [1985] and the references therein) and two questions immediately arise: the importance of non-gyrotropic electrons in the upstream and the validity of the observations in the original paper.

The *Anderson et al.*, [1985] paper contained numerous examples of upstream electron events but for only one event were the velocities and temperatures derived to show that the distribution was non-gyrotropic. For that event the temperature was roughly 40 eV and the average energy on the order of 3 keV. These values were not direct observations but arrived at through a deconvolution of the spin modulations observed in the data. That has left some doubt as to the uniqueness of the solution.

The large electron energy makes it unlikely that that the observed non-gyrotropic electron distribution was produced by a reflection of the solar wind off of the shock front; one mechanism known to produce non-gyrotropic ions. In the reflection process the incident velocity is repartitioned between the parallel and perpendicular components giving rise to a displacement of the particle guiding center with respect to the interplanetary electric field. This produces an acceleration in the perpendicular direction which if large enough bunches the reflected solar wind in phase. The energization available depends in part on the gyroradius of the incident particle; the larger the gyroradius the higher the possible energy gain. The reflection process does not have the potential to accelerate solar wind electrons up to the keV energy range.

A second mechanism known to gyrophase-bunch ions in the upstream is resonant trapping by MHD waves [*Fuselier et al.*, 1986; *Gary et al.*, 1986]. A similar mechanism would be a more likely source for the electron observations. *Anderson et al.* [1985] realized that phase-trapping was a necessary condition for gyrophase-bunched electron observations. Without it the high electron gyrofrequency would effectively gyrophase mix the distribution into a ring-beam before any measurement could be completed [*Gurgiolo et al.*, 1983; *Burgess and Schwartz*, 1984].

The importance of non-gyrotropic electron distributions in the upstream is not fully understood or appreciated at this time. It is possible that they may be the source of the upstream ion acoustic emissions. The mechanism for generating the ion acoustic wave in the upstream is still open. It is interesting to note that high-frequency whistler waves have been shown in simulations to exist ahead of the MHD waves generated by gyrophase-bunched ion distributions in the upstream [*Gurgiolo et al.*, 1993] and that these regions have been shown to be strongly correlated with ion acoustic waves [*Parks et al.*, 1995; *Anderson et al.*, 1981]. It remains to be seen if these regions are also associated with non-gyrotropic electrons.

This paper presents an initial set of observations of a gyrophase-bunched electron signature found in the upstream. The distributions were observed following two traversals of the bow-shock.

The data were obtained from the University of California at Berkeley low energy electron electrostatic analyzer experiment (EESA-LOW), part of the ISTP WIND 3-D Plasma and Energetic Particle Experiment [*Lin et al.*, 1995]. Briefly, EESA-LOW is a quadrespherical analyzer measuring electrons in elevation from -90° to 90°. It is mounted on a 0.5 meter boom to isolate it from spacecraft charging effects. Azimuthal coverage is provided by the satellite rotation giving a full 3D distribution in 3 seconds. During the time presented in this paper, the instrument was returning data in 32 azimuthal bins, 8 elevation bins and in energy from 8 eV to 1.15 keV in 15 equally spaced logarithmic steps. Each azimuthal slice through the distribution takes roughly 93 ms to complete. Although a full 3-D distribution is accumulated each 3 seconds only one distribution of each 16 taken was being telemetered to the ground. This severely decimates the data in time.

Paper number 2000GL000065.
0094-8276/00/2000GL000065$05.00

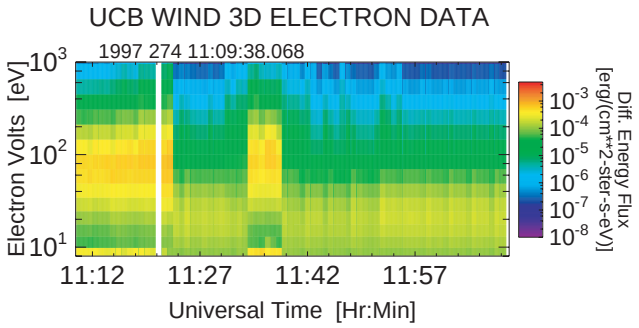

Figure 1. Spectrogram detailing the plasma environment surrounding the time of the observed non-gyrotropic electron distributions. See text for more details.

Observations

Figure 1 shows an overview of the period of interest. The data from all 8 polar elevations have been averaged to form a single spectrogram. Data is displayed as differential energy flux (ergs/cm^2-ster-s-eV) and color-coded according to the color bar at the right. Gaps in the data created by the temporal decimation have been smoothed over.

The plot begins with the satellite in the magnetosheath-shock. Near 11:23:00 UT the shock is crossed and the satellite enters the upstream. There is a short excursion back into the magnetosheath-shock region beginning at 11:33:30 UT with the satellite re-entering the upstream at 11:37:45 UT No further encounters with the shock are observed in the outbound pass. The gyrophase bunched distributions are observed prior to the entry into and after the exit from the last encounter with the shock.

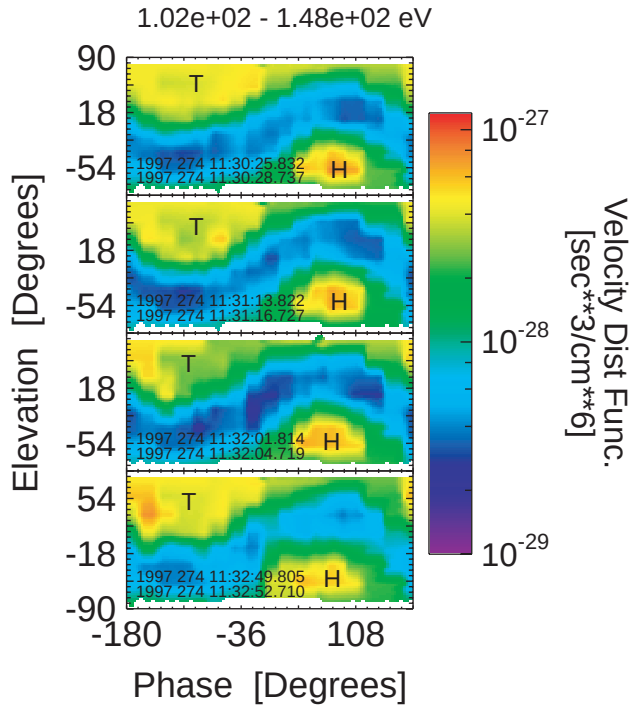

Figure 2. GSE elevation/phase plots leading up to the shock crossing near 11:33:30 UT. Distribution shown is between 102 and 148 eV. The return distribution in the upper left begins to exhibit non-gyrotropic features beginning in the second plot. See text for more details.

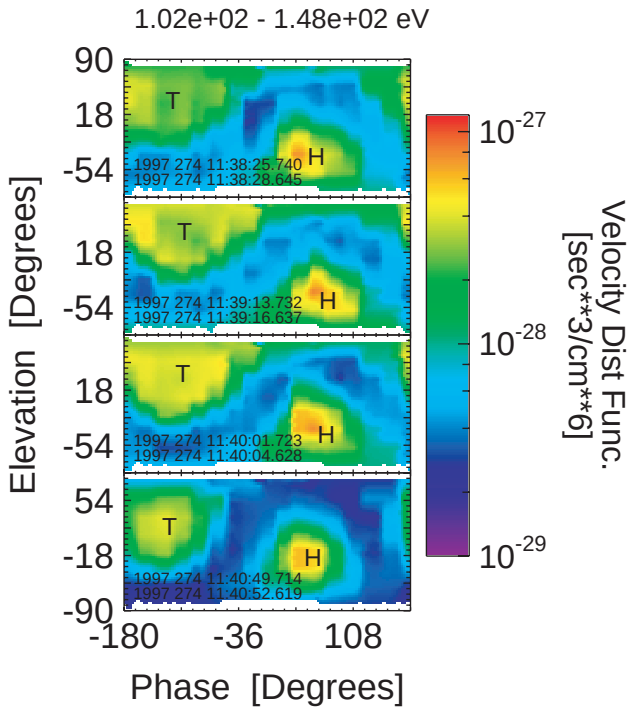

Figure 3. Follow up to Figure 2 with the plots picking up immediately after the satellite re-enters the upstream at 11:37:45 UT. The initial 2 return distributions are similar to the distributions seen prior to entering the shock, although weaker in intensity.

Figures 2 and 3 show a progression of the electron distribution in the upstream just prior to entering the shock and again just after entering back into the upstream. Each plot shows one instance of the electron velocity distribution (sec^3/cm^6) between the energies of 102 and 148 eV (the phase space density within a shell in velocity space bounded by the energies 102 and 148 eV) as a function of GSE phase and elevation.

The data have been corrected to the plasma rest frame by subtracting off the ion solar wind velocity. This has negligible effect on the electron energy but effects the angular distribution of the data. The change in phase and elevation vary with angle and can be as high as 7°. The error in the final angle is proportional to the error in the measured solar wind velocity.

The corrected data is plotted on a rectangular grid and then passed through a contouring filter for the final plot. Plots were produced for a number of different energy ranges. The features shown are present from about 70 to 350 eV. Below 70 eV the distribution is dominated by the core electrons. Above 350 eV the coarse distribution features remain but there can be shifts in the phase of the return electron signature.

The H and T in each plot are the projection of head and tail of the average magnetic field vector. The upstream magnetic field for both sets of plots had a magnitude of roughly 8.5 nT with a strong Z component as evidenced by the projections.

Two distinct electron components can be identified in each of the 8 plots. The enhancement consistently seen in the lower right of the plots is a field-aligned beam moving towards the shock and is referred to as the "incident electron

distribution" in the text. In the upper left of the plots is a general field-centered electron distribution moving away from the shock, referred to as the "return distribution" in the text. It is the return distribution which at times becomes non-gyrotropic.

Discussion

Each plot in Figures 2 and 3 covers one spin's worth of data; about 3 seconds or 700 electron gyroperiods. The latter number far exceeds the "snapshot" criterion required to distinguish a freely rotating gyrophase-bunched distribution and any non-gyrotropic features observed in the plots must be the result of a locally phase-standing distribution.

Prior to claiming that any observed distribution is the result of gyrophase-bunching, the effects of temporal and spatial variations in the data need be addressed as both may at times introduce non-gyrotropic appearing features. Temporal variations in the data which occur on time scales shorter than the measurement period can produce a false non-gyrotropic signature. In the UCB data temporal changes affect all data within a fixed phase bin; all elevation data at a fixed phase being taken simultaneously. If the variation has a long enough duration it can extend across phase bins. Variations which are highly localized in elevation will show up as bright spots in the plots. Unless localized features are sustained or exhibit a clear progression in phase over multiple plots they are considered transient and for the purpose of this paper they are ignored. The isolated bright spot in the second plot in Figure 2 at $\phi = -55^\circ$ may be an example of a local temporal enhancement.

In addition to rapid intensity fluctuations there can also be gradual increases or decreases in the overall intensity. This generally does not affect a non-gyrotropic signature in the data but is a good measure of the stability of the distribution over the observation period. Changes of this kind should manifest themselves near a phase of 33° in the plots. The data on either side of this line differ in time by 3 seconds.

Spatial variations in the data can both destroy and mimic non-gyrotropic features. A gyrophase-bunched distribution from a point source is helical in space. Satellite movement along the cylindrical axis of the helix can spread the measured phase to a point where it appears to be a ring-beam. The actual spread in measured phase due to satellite motion can be estimated by

$$\phi = \frac{360 V_s t cos\theta}{\lambda} \quad (1)$$

where V_s is the satellite velocity, t is the integrated measurement time, θ is the angle between the spacecraft velocity and the cylindrical axis of the helix, and λ is the helix wavelength. For this data V_s is 2.5 km/sec, and t measured to be about 1.25 seconds (150°) for the return distribution. λ is unknown but a value in the range 10 to 30 km is probably not out of line, this being comparable to the whistler wavelength. Taking λ as 10km and θ as 0° (both worst case values) gives a spread in phase of 112.5°; a value not high enough to entirely destroy any phase-bunching signatures but large enough to smear the distribution to the point that nothing should be made its spread in the phase.

Finite gyroradius effects, which are spatial in nature, may produce non-gyrotropic signatures in the data. These can occur in measurements made within a gyroradius of large gradients in the particle density. For the particle energy plotted the gyroradius is about 35 km and while the satellite only moves about 6 km in one spin, there is 45 seconds of dead time between between plots and the satellite travels almost 110 km between plots. It is unlikely that a sustained finite gyroradius signature exists in the data.

Temporal variations in the magnetic field within the time of the measurement of the return distribution may smear the distribution. This variation can be represented as a wobble in the vector head and tail in the plots. For the third plot in Figure 2 this wobble amounts to -93 to -111° in phase and 44 to 52° in elevation in the vector tail. For the bottom plot the values are -90 to -120° in phase and 33 to 61° in elevation. Neither set of wobbles are large enough to sufficiently effect the observed non-gyrotropic signature.

Lastly, spacecraft charging must always be considered. This can be ruled out on the basis of the energy range and from the fact that the data is ordered by the magnetic field. Spacecraft produced photoelectrons may reach this energy but produce a distribution peaked at a pitch angle of 90° and would not extend to the higher energy bands looked at.

With the above discussion as background, the plots in both Figures 2 and 3 can be examined. The first evidence of a return distribution is in the top plot in Figure 2. There is no evidence of a return distribution prior to that time. The first return distribution resembles a ring-beam. There is probably no variation of the distribution about the ring that could not be attributed to statistics. Beginning, however, with the next plot things change. A portion of the left side of the return distribution begins to brighten, the trend continuing through the next two plots. The location of the enhancement remains about the same in each plot. The original ring is almost always observable as a low-level background.

The enhancement is still present in the first two plots in Figure 3 when the satellite re-enters the upstream. By the third plot the return distribution has the original ring-beam signature and by the fourth plot is a field-aligned beam. This last signature persists for one plot beyond the last shown. After that there is no longer any evidence of a return distribution.

The persistence of the enhancement in the last three plots in Figure 2 and the first two in Figure 3 coupled with the similarity of the signature in each plot (remember successive plots are separated by 45 seconds in time) is strong evidence that this is not a temporal or finite gyroradius feature. The return distribution in all of these plots is non-gyrotropic with respect to the three second averaged magnetic field.

The progression seen in the distributions is consistent with what might be expected for a source of gyrophase particles near the shock. With increased distance from the source, the distribution goes from gyrophase bunched to ring-beam to pure beam, scattering in phase being much more efficient that scattering in energy. The same progression was observed in the velocity distributions of cometary protons pickup by solar wind at Comet Halley shock [*Neugebauer et al.*, 1989].

At the present the mechanism for producing gyrophase-bunched electrons in the upstream is unknown. Phase trapping must occur after the fact. The energy range at which the gyrophase-bunched electrons are observed would seem to rule out specular reflection at the shock as the source. What role, if any in fact, the shock plays in this process is not known. Further information on the exact mechanism(s)

responsible for the production of gyrophase bunched electron distributions in the upstream, their frequency of occurrence, and what if any role they play will await a more systematic and thorough investigation as well as the inclusion of detailed simulation results.

Acknowledgment. CG and HKW would like to acknowledge support by NASA Contract NAS5-6099. CG would also like to acknowledge and thank Ron Lepping for the use of the high resolution magnetometer data.

References

Anderson, K. A., et al, A component of nongyrotropic (phase-bunched) electrons upstream from the earth's bow shock, *J. Geophys. Res., 90,* 10809, 1985.

Anderson, R. R., et al., Plasma waves associated with energetic particles streaming into the solar wind from the earth's bow shock, *J. Geophys. Res., 86,* 4493, 1981.

Burgess, D. and S. J. Schwartz, The dynamics and upstream distributions of ions reflected at the Earth's bow shock, *J. Geophys. Res., 89,* 7407, 1984.

Fuselier, S. A., et al., The phase relationship between gyrophase-bunched ions and MHD-like waves. *Geophys. Res. Lett., 13,* 60, 1986.

Gary, S. Peter., et al., Computer simulations of electromagnetic cool ion beam instabilities. *J. Geophys. Res., 91,* 4188, 1986.

Gurgiolo, C., G. K. Parks, and B. H. Mauk, Upstream gyrophase bunched ions: A mechanism for creation at the bow shock and the growth of velocity space structure through gyrophase mixing, *J. Geophys. Res., 88,* 9093, 1983.

Gurgiolo, C., H. K. Wong, and D. Winske, Low and high frequency waves generated by gyrophase-bunched ions at oblique shocks, *Geophys. Res. Lett., 20,* 783, 1993.

Lin, R. P., et al., A three-dimensional plasma and energetic particle investigation for the wind spacecraft. *Space Sci. Rev., 71,* 122-153, 1995.

Neugebauer, M., et al., The velocity distributions of cometary protons picked up by the solar wind. *J. Geophys. Res., 94,* 5227, 1989.

Parks, G. K., et al, Upstream particle gradients and plasma waves, *J. Geophys. Res., 20,* 4343, 1981.

Thomsen, M. F., Upstream suprathermal ions, in *Collisionless Collisionless Shocks in the Heliosphere: Reviews of Current Research,* edited by B. T. Tsurutani and R. G. Stone, AGU, Washington D. C., 253, 1985.

C. Gurgiolo, Bitterroot Basic Research Inc. 837 Westside Road Hamilton, MT 59840 (e-mail: chrisg@cybernet1.com)

D. Larson and R. P Lin, Department of Space Science, University of California at Berkeley Berkeley, CA 94720 (e-mail: davin@sunspot.ssl.berkeley.edu; rlin@sunspot.ssl.berkeley.edu)

H. K. Wong, Aurora Science, 4502 Centerview Dr., STE 120 San Antonio, TX 78228 (e-mail: kit@cascade.gsfc.nasa.gov)

(Received March 21, 2000; revised July 12, 2000;
accepted July 28, 2000.)